

The Two Positively Acting Regulatory Proteins PHO2 and PHO4 Physically Interact with *PHO5* Upstream Activation Regions

KURT VOGEL,¹ WOLFRAM HÖRZ,² AND ALBERT HINNEN^{1*}

Biotechnology Department, CIBA-GEIGY AG, CH-4002 Basel, Switzerland,¹ and Institut für Physiologische Chemie, Physikalische Biochemie, und Zellbiologie der Universität München, 8000 Munich 2, Federal Republic of Germany

Received 12 September 1988/Accepted 7 February 1989

The repressible acid phosphatase gene *PHO5* of *Saccharomyces cerevisiae* requires the two positively acting regulatory proteins PHO2 and PHO4 for expression. *pho2* or *pho4* mutants are not able to derepress the *PHO5* gene under low- P_i conditions. Here we show that both PHO2 and PHO4 bind specifically to the *PHO5* promoter in vitro. Gel retardation assays using promoter deletions revealed two regions involved in PHO4 binding. Further characterization by DNase I footprinting showed two protected areas, one located at -347 to -373 (relative to the ATG initiator codon) (UAS_p,1) and the other located at -239 to -262 (UAS_p,2). Exonuclease III footprint experiments revealed stops at -349 and -368 (UAS_p,1) as well as at -245 and -260 (UAS_p,2). Gel retardation assays with the PHO2 protein revealed a binding region that lay between the two PHO4-binding sites. DNase I footprint analysis suggested a PHO2-binding site covering the region between -277 and -296.

The promoter region of the strongly regulated acid phosphatase gene *PHO5* (4) has been recently analyzed by deletion mapping (6, 19, 24). In addition to the TATA box, two regions were found (24) to be essential for activation of the *PHO5* promoter. Sequence comparisons defined four elements from which a 19-base-pair dyad consensus sequence was deduced. Three of the elements, called UAS_p, were located within deletions showing reduced transcription of *PHO5* (24), at -367, -245, and -185 relative to the translational start.

Not much is known about the physical interaction of regulatory proteins with the *PHO5* promoter. Since mutations defective in *PHO2* or *PHO4* are epistatic to all other regulatory mutations and show a negative phenotype, it is likely that the PHO2 and PHO4 proteins are positive transcription factors that interact with the *PHO5* promoter DNA. The finding that a *pho2* mutation can be complemented by overexpression of the PHO4 protein (20) is a further indication that the PHO2 and PHO4 proteins exert their functions at the same late hierarchical level of *PHO5* activation.

Extensive studies of the chromatin fine structure of the *PHO5* gene (1, 2, 5, 7) have been done. Interestingly, the element at -367, which is essential for gene induction (24), resides in the center of a hypersensitive region under conditions of *PHO5* repression (1, 2).

In this paper, we show that the two positive regulatory proteins PHO4 and PHO2 bind specifically to *PHO5* promoter DNA. Footprint analysis revealed two regions (UAS_p,1 and UAS_p,2) protected by the PHO4 protein. The *PHO5* promoter was found to have a PHO2-binding site located between the two PHO4-binding sites. These results are in agreement with data obtained by our fine-structure deletion mapping (24) but differ to some extent from data published by Nakao et al. (19) and Bergman et al. (6).

Recently, it was shown that BAS2 (allelic to PHO2) also binds to the *HIS4* promoter region (3) and regulates the basal level of *HIS4* expression. Furthermore, PHO2 was found to bind very strongly to the *TRP4* promoter (G. Braus, H.-U. Mösch, K. Vogel, A. Hinnen, and R. Hütter, EMBO J., in

press). Interestingly, the *pho2* mutation showed no influence on the basal level of *TRP4* expression but rather modulated the general control response of *TRP4*.

MATERIALS AND METHODS

***Escherichia coli* vector for *PHO4* and *PHO2* expression.** The *PHO4* gene (13, 15) was reisolated from a S288C background by screening an ordered centromere library (25). An *Nco*I site at the ATG of *PHO4* was introduced by site-specific mutagenesis (14). The *PHO4* gene (*Nco*I-*Bam*HI fragment) was placed under control of the inducible p_L promoter by using the vector pPLmu, a derivative of PLc24 (23) containing the phage Mu Ner gene ribosome-binding site with an *Nco*I site at its ATG start codon (obtained from Biogen).

The *PHO2* gene (25) was fused to the same vector but carrying a different ribosome-binding site (no. 27-4878-01 and 27-4898-01; Pharmacia, Uppsala, Sweden; vector kindly provided by A. Schmitz). The correct fusion of this ribosome-binding site to the *PHO2* gene was achieved with an adapter oligonucleotide that fits to the *Bam*HI site of the ribosome-binding site and the *Eco*RI site of the *PHO2* gene. The correct in-frame fusions of both constructions were verified by sequencing the junctions.

Partial purification of *E. coli*-expressed PHO4 and PHO2 proteins. The *E. coli* expression vector with the *PHO4* or *PHO2* genes was transformed into JM109 cells carrying the temperature-sensitive λ repressor pc1857 on a plasmid. Upon heat induction, heterologous protein accumulated to a few percent of the level of total cellular protein. For binding studies, a soluble cell lysate (1.2 g of total protein for PHO4 and 0.5 g for PHO2) was partially purified by applying it to a DE-52 column (30-ml bed volume) in 100 mM Tris (pH 7.5)-0.1 mM EDTA-1 mM phenylmethylsulfonyl fluoride and rinsing the preparation with the same buffer. The flowthrough fractions were passed through an Affi-Gel-heparin (Bio-Rad Laboratories, Richmond, Calif.) column (30-ml bed volume). Protein was eluted from the heparin-sepharose column by applying a Tris gradient. The pooled fractions contained approximately 10% PHO4 and 2% PHO2, respectively.

Gel retardation assays. For gel retardation assays (10), the recessed 3' ends of the DNA fragments were filled in with

* Corresponding author.

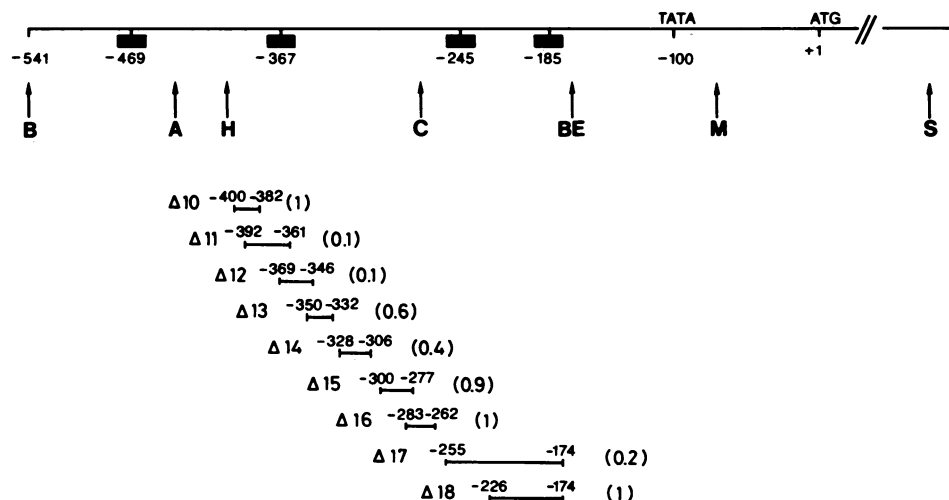


FIG. 1. The *PHO5* promoter. Negative numbers indicate elements found by deletion mapping (24). Listed beneath the sequence are some of the deletions used. Numbers in brackets show activities of the deletions in vivo. Restriction sites: A, *Aat*II; B, *Bam*HI; BE, *Bst*EII; C, *Cla*I; H, *Hin*PI; M, *Mn*II; S, *Sal*I.

Klenow polymerase as described by Maniatis et al. (17), using α - 35 S-labeled deoxynucleoside triphosphates. Approximately 1 ng of labeled fragments was added to a 20- μ l (final volume) reaction mixture containing 100 mM NaCl, 10 mM Tris (pH 7.5), 2 mM dithiothreitol, 0.1 mM EDTA, and 2 μ g of double-stranded poly(dI-dC) competitor DNA. Finally, 0.2 μ g of PHO4 or 2 μ g of PHO2 protein (partially purified) was added, and the binding reaction was allowed to proceed for 15 min at 25°C. The samples were loaded immediately (under voltage) onto a 6% polyacrylamide gel (acrylamide-bisacrylamide weight ratio of 30:1) made in 0.5 \times TBE. (50 mM Tris [pH 8.3], 50 mM boric acid, and 1.25 mM EDTA). Electrophoresis was performed at 350 V for 2 to 3 h at room temperature. The dried gels were exposed to sensitive X-ray films (Eastman Kodak Co., Rochester, N.Y.).

DNase I footprinting with PHO4. DNase I footprint assays were adapted from the method of Galas and Schmitz (9). A 32 P-end-labeled DNA fragment (approximately 20,000 Cerenkov counts) was added to 20 μ l (final volume) of reaction mixture containing 50 mM NaCl, 10 mM Tris (pH 7.5), 2 mM dithiothreitol, 1 mM EDTA, 0.5 mM MgCl₂, and 1.5 μ g of poly(dI-dC) competitor DNA. After addition of 0.5 μ g of partially purified PHO4 protein, the binding reaction was allowed to proceed for 15 min at 25°C. The samples were transferred on ice, and 2 μ l of DNase I (50 μ g/ml) freshly diluted in 10 mM Tris (pH 7.5)–25 mM CaCl₂ was added to the reaction mixtures. Digestion with DNase I was allowed to proceed for 3 min on ice. The samples were loaded on a standard sequencing gel.

DNase I footprinting with PHO2. DNase I footprint assays were done as described for PHO4 except that protein-DNA complexes were prepared with 5 μ g of partially purified PHO2 protein in the presence of 100 mM NaCl and the reaction volume was scaled up to 50 μ l, containing approximately 200,000 to 400,000 Cerenkov counts per sample. After DNase I treatment, 10 μ l of 0.2 M EDTA (pH 7.5) was added. The samples were loaded immediately onto a 6% native polyacrylamide gel as described for gel retardation assays. The wet gels were exposed to X-ray films, and the two protein-specific complexes were isolated from the gel and loaded onto a standard sequencing gel.

Exonuclease III footprinting. For protein-DNA binding, a 32 P-end-labeled fragment (approximately 20,000 Cerenkov

counts) was added to 38 μ l (final volume) of reaction mixture containing 50 mM NaCl, 10 mM Tris (pH 7.5), 2 mM dithiothreitol, 5 mM MgCl₂, 0.1 mM EDTA, and 3 μ g of double-stranded poly(dI-dC) competitor DNA. Then 1 μ g of partially purified PHO4 protein was added. After the binding reaction was allowed to proceed for 15 min at 25°C, 2 μ l (12.5 U) of exonuclease III (Boehringer Mannheim Biochemicals, Indianapolis, Ind.) was added for 3, 6, or 12 min at 25°C. The reaction was stopped by addition of 4.8 μ l of 500 mM Tris (pH 8.0)–50 mM EDTA–5% sodium dodecyl sulfate and 2 μ l of proteinase K (10 mg/ml). After proteinase K treatment, the samples were loaded onto a standard sequencing gel.

RESULTS

PHO4 and PHO2 proteins bind specifically to the *PHO5* promoter. The promoter region of *PHO5* was screened for functionally important DNA sequences by the construction of a series of deletion mutants (24) (Fig. 1). To determine whether the regulatory proteins PHO2 or PHO4 bound directly to the *PHO5* promoter, we decided to analyze this possible protein-DNA interaction in vitro. Both proteins were expressed in *E. coli* (see Materials and Methods), which eliminated the possibility of contamination by other yeast proteins. After partial purification of the expressed proteins, gel retardation experiments were performed with *PHO5* promoter DNA. Radiolabeled DNA fragments were incubated with the regulatory proteins and subjected to native polyacrylamide gel electrophoresis as described in Materials and Methods. The presence of the PHO4 protein changed the mobility of the wild-type promoter fragment (Fig. 2). Distinct complexes migrating with a lower mobility than that of the free DNA were observed. The interaction with *PHO5* promoter DNA was specific, since no binding was observed with a control DNA fragment (Fig. 2, lane c) representing part of the *PHO5* coding region.

The observed complexes appeared as two sets of triplet bands (Fig. 2). The individual bands within each triplet set consistently showed decreasing intensity with increasing mobility, which suggested different stabilities of the various complexes. Figure 2 also shows protein-DNA complexes with promoter fragments that harbored internal deletions (Δ 7 to Δ 20; Fig. 1). Most of these produced the same pattern as



FIG. 2. Localization of PHO4-binding sites to the *PHO5* promoter. Gel retardation assays were performed as described in Materials and Methods with ^{35}S -labeled *Bam*HI-*Bst*EII promoter fragments. The deletions ($\Delta 10$ to $\Delta 18$) are shown in Fig. 1. wt, Wild-type *PHO5* promoter fragment; c, a 370-base-pair fragment from the *PHO5* coding region used as a negative control. The fastest-moving bands represent free DNA fragments.

did the wild-type fragment, which indicated that a particular deletion did not interfere with PHO4 binding. However, $\Delta 11$, $\Delta 12$, and $\Delta 17$ showed only one set of triplet bands, which suggested that one binding area for the PHO4 protein was missing. This finding coincides with the *in vivo* data, which showed that $\Delta 11$, $\Delta 12$, and $\Delta 17$ led to a reduced level of *PHO5* mRNA (24). The observed triplet pattern could also be explained as containing partially degraded PHO4 protein. However, the regular spacing of the single bands would imply a specific kind of degradation, which is unlikely.

It is interesting that deletion $\Delta 7$, missing the element at -469 , did not influence the gel retardation pattern. This finding is in complete agreement with our *in vivo* data showing that deletion $\Delta 7$ produced no decrease in *PHO5* mRNA expression. Thus, the element at -469 must be considered a fortuitous sequence with no biological significance.

After the same gel retardation assay was done with partially purified PHO2 protein, a significantly different pattern of complexes was obtained. The PHO2 protein yielded a double band on a native polyacrylamide gel (Fig. 3). As was observed with the PHO4 protein, the binding of PHO2 was specific for *PHO5* UAS DNA and did not occur with the control fragment. Fragments $\Delta 15$ and $\Delta 16$ did not bind PHO2 protein, as judged by the absence of either complex. This region obviously contains a sequence involved in PHO2 binding. Unexpectedly, the deletions $\Delta 15$ and $\Delta 16$ showed only minor or no effects on *PHO5* mRNA expression *in vivo*.

PHO4 protein protects two regions against DNase I. The PHO4-binding sites defined by deletions $\Delta 11$, $\Delta 12$, and $\Delta 17$ were more precisely analyzed by DNase I protection experiments (9) as described in Materials and Methods. In brief, the *Aat*II-*Bst*EII fragment of *PHO5* promoter DNA (Fig. 1) was radioactively labeled at either 5' end and incubated with the PHO4 protein. Protein-DNA complexes were treated briefly with DNase I. Proteins were subsequently digested with proteinase K, and the DNA was electrophoresed on a standard sequencing gel.



FIG. 3. Localization of PHO2-binding sites to the *PHO5* promoter. Assay conditions and fragments were as for Fig. 2. The fastest-moving bands represent free DNA, the middle band is complex 1, and the slowest band is complex 2.

Two regions, from -347 to -373 (UAS_{p1}) and from -245 to -262 (UAS_{p2}) (see Fig. 6A and C), were protected by the PHO4 protein against DNase I digestion (Fig. 4). Deletions $\Delta 11$, $\Delta 12$, and $\Delta 17$ deleted DNA sequences from -362 to -392 , -346 to -369 , and -174 to -255 , respectively (24), and overlapped perfectly with the two protected segments. DNase I footprint analysis using the *Bam*HI-*Bst*EII or *Aat*II-*Mnl*I *PHO5* promoter DNA fragment (Fig. 1) showed no protected regions different from UAS_{p1} and UAS_{p2} (data not shown), which indicated that the elements at -469 and -185 are not involved in PHO4 binding even though they fit the consensus sequence (24) quite well. Our data argue strongly that PHO4-mediated activation of the *PHO5* gene occurs only via the two PHO4-binding sites UAS_{p1} and UAS_{p2}. Furthermore, we could not detect by gel retardation assays and footprints any influence on PHO4 binding of the presence of ATP, cAMP, or P_i in the binding reaction (data not shown).

Determination of the exact boundaries of the PHO4-binding sites by exonuclease III digestion. Exonuclease III footprinting revealed a more precise footprint than did DNase I. In brief, 5'-radiolabeled DNA fragments were incubated for different periods of time with exonuclease III in the presence and absence of the PHO4 protein. Stable protein-DNA complexes do not allow exonuclease III to digest DNA within and downstream of the complex. This interference will produce (radioactive) DNA fragments of particular lengths that can be resolved on sequencing gels. Individual exonuclease III digests from either end of a fragment define the left and right borders of a binding site involved in protein-DNA interaction.

Figure 5 shows the pattern obtained upon digestion of the *Aat*II-*Bst*EII fragment unidirectionally by exonuclease III, starting at the *Bst*EII site (Fig. 5A). In the absence of the PHO4 protein, the fragment became gradually degraded with increasing incubation time. Some preferential stops that might be explained by colliding exonuclease III molecules appeared after 6 min of digestion. However, in the presence of the PHO4 protein, a very strong exonuclease III stop was observed at -245 , the site of UAS_{p2}. In particular, it was interesting to note that no exonuclease III stop at UAS_{p1}, which would result in a specific radioactive fragment with higher electrophoretic mobility, was observed.

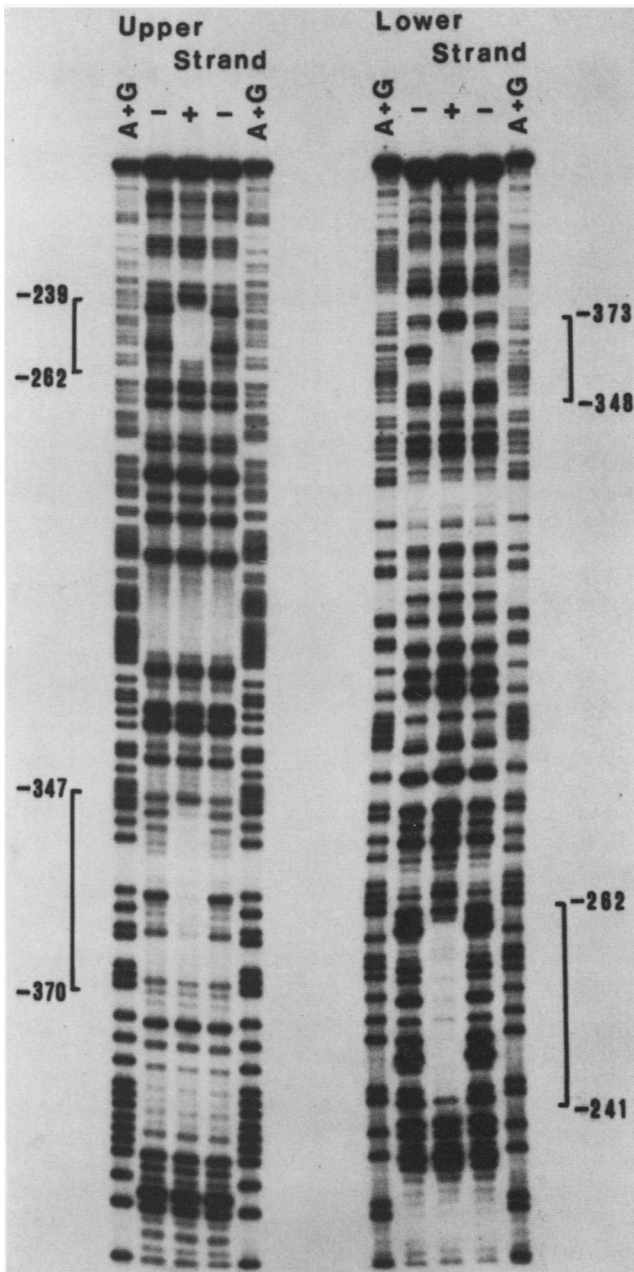


FIG. 4. DNase I footprint analysis with the PHO4 protein. DNase I footprinting was performed as described in Materials and Methods. The upper strand was labeled at the *AatII* site, and DNA was restricted with *BstEII* to generate the 270-base-pair fragment containing UAS_p1 and UAS_p2 . The lower strand was labeled at the *BstEII* site and restricted with *AatII*. The DNA probes were incubated in the presence of poly(dI-dC) competitor DNA with (+) or without (-) the PHO4 protein for 15 min and treated as described in Materials and Methods. A+G, Maxam-Gilbert sequencing reactions (18) of the same DNA fragments used as size markers.

On the other hand, exonuclease III digestion starting at the *Clal* site (Fig. 5B) resulted in a specific stop at -349, the UAS_p1 site (note that the *AatII-Clal* fragment lacked UAS_p2). Furthermore, the digestion pattern of the complementary strand generated by labeling of the *BstEII* site and digestion from the *HinPI* site (Fig. 5C) showed two prominent exonuclease III stops. A short digestion resulted in a

specific exonuclease III stop at -368 that disappeared upon longer digestion. After 12 min of digestion, however, a prominent stop occurred at -260, the UAS_p2 site.

The fact that no further digestion at -245 (UAS_p2) was obtained even after 12 min of incubation, whereas free DNA was almost completely digested, argues that the two sites behave in a distinctive manner with respect to PHO4 binding. This observation could be confirmed by DNase I footprinting, using various amounts of partially purified PHO4 protein. At low PHO4 concentrations, UAS_p1 was barely protected whereas UAS_p2 was fully protected (data not shown).

Figure 6A summarizes the protected sequences obtained by DNase I and exonuclease III footprinting. The two sequences showed little homology to each other except for the pentamer CACGT, in approximately the middle of each UAS_p .

PHO2 protein binds to a region between the PHO4-binding sites. Having shown by gel retardation experiments (see above) that the PHO2 protein binds specifically to a region between UAS_p1 and UAS_p2 , resulting in two characteristic complexes, we became more interested in the nature of these complexes. We therefore combined gel retardation and DNase I footprinting to study the complexes in more detail. *AatII-BstEII* restriction fragments were labeled at either end and treated with DNase I in the presence or absence of the PHO2 protein. Free DNA and the two complexes were resolved and recovered from a native polyacrylamide gel. DNA was then subjected to denaturing polyacrylamide gel electrophoresis (see Materials and Methods).

In comparison with free DNA, the DNA present in complex 1 (the faster-moving protein-DNA complex) showed a protein-DNA interaction between -277 and -296 (Fig. 7B), recognized as a pattern of bands of different intensities. Unlike the footprint obtained with the PHO4 protein, PHO2 interaction also resulted in hypersensitive sites.

The same DNA region was involved in the protein-DNA interaction resulting in the formation of complex 2, the slower-moving complex. This finding indicates that PHO2 does not bind as a single molecule but rather forms higher-order complexes such as dimers or tetramers. This finding was confirmed by the observation that $\Delta 15$, which removed the PHO2-binding site, led to the disappearance of the two complexes (Fig. 3). Also, $\Delta 16$ showed no PHO2 binding (Fig. 3) and therefore must contain sequences important for protein-DNA interaction. The additional changes in intensity of some bands, seen in complex 2 (Fig. 7B), could be explained by higher-order structures of PHO2; alternatively, PHO2 may bind to a second binding site, since we have some indications that PHO2 can interact with adjacent sequences partially overlapping UAS_p2 .

Obviously, the protein-DNA interaction for PHO2 is much weaker than that for PHO4. We have not been able to stabilize the complexes by adding ATP, cAMP, P_i , or zinc ions to the binding reaction. Furthermore, the presence of the PHO4 protein in the binding reaction did not improve the PHO2-DNA interaction, which suggests that PHO4 and PHO2 bind independently to the two UAS elements of the *PHO5* promoter.

DISCUSSION

Our protein-DNA interaction studies have shown that PHO2 and PHO4 bind specifically to the *PHO5* promoter DNA. Gel retardation experiments showed that two regions on the *PHO5* promoter, defined by $\Delta 11$ - $\Delta 12$ and $\Delta 17$ (Fig.

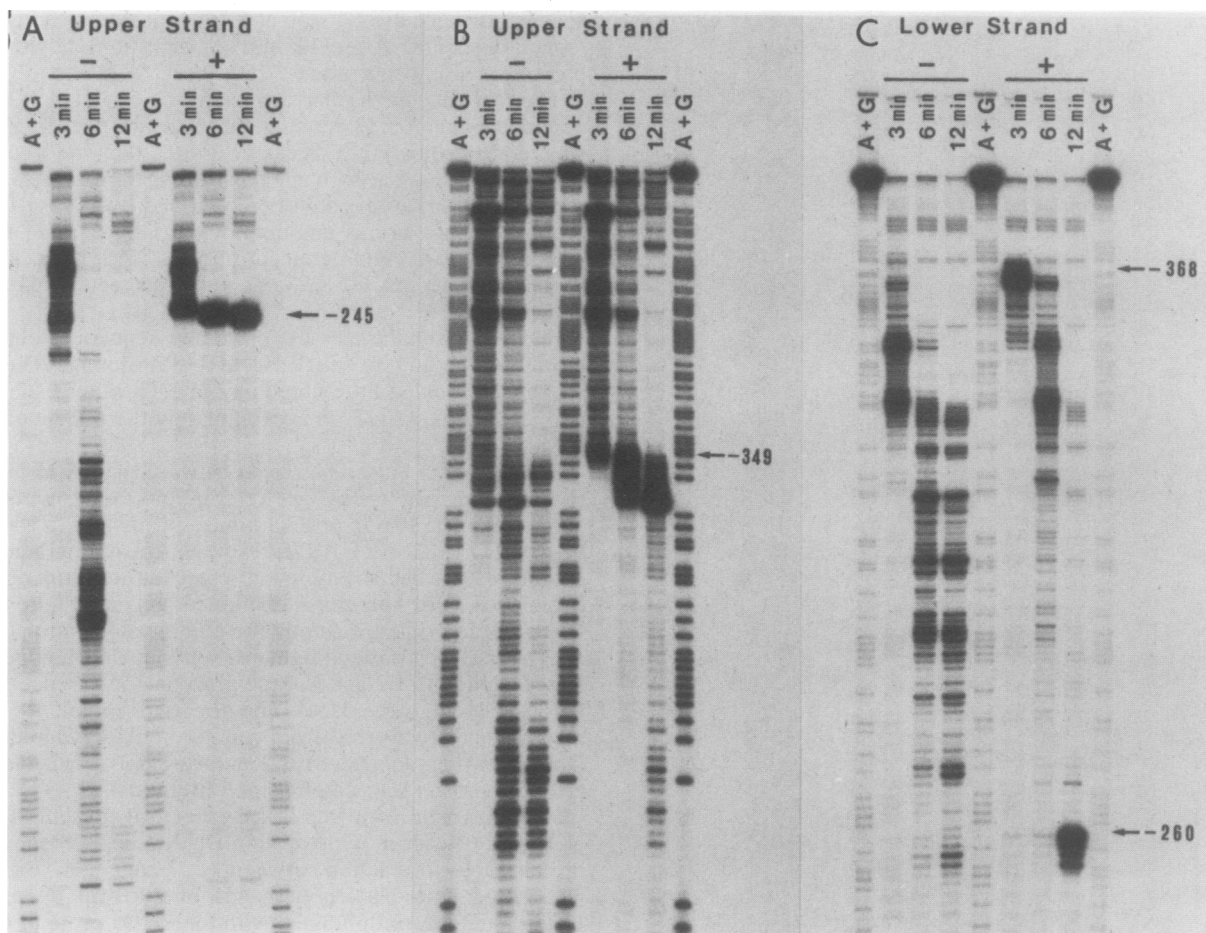


FIG. 5. Exonuclease III footprint analysis with the PHO4 protein. Exonuclease III footprinting was performed as described in Materials and Methods. The upper strand was labeled at the *Aat*III site and digested with exonuclease III from the *Bst*EII site (A) or from the *Cla*I site (B). The *Aat*III-*Bst*EII fragment contains UAS_p1 and UAS_p2, whereas the *Aat*III-*Cla*I fragment contains only UAS_p1. The lower strand was labeled at the *Bst*EII site and exonuclease III digested from the *Hin*PI site (C). The DNA probes were incubated in the presence poly(dI-dC) competitor DNA with (+) or without (-) the PHO4 protein for 15 min and digested with 12.5 U of exonuclease III per assay for 3, 6, and 12 min. A+G, Maxam-Gilbert sequencing reactions (18) used as size markers.

6C), are involved in PHO4 binding and that another region, defined by $\Delta 15$ and $\Delta 16$, is involved in PHO2 binding. Footprint analysis mapped the PHO4-binding sites at -347 to -373 (UAS_p1) and at -239 to -262 (UAS_p2) (Fig. 6A and C), and exonuclease III stops defined binding regions at -349 to -368 and at -245 to -260. These PHO4-binding sites are in good agreement with the phosphate control sequences defined previously (24).

The PHO2 protein was found to occupy one region, between -277 and -296 (Fig. 6B and C). The footprint data for PHO2 showed that complex 1 as well as complex 2 (Fig. 3) protected approximately the same area (Fig. 7). The different intensities of some additional bands in complex 2 (lower strand) could have resulted from the higher-complex formation of the PHO2 protein. More interesting, we have some indications that PHO2 may bind in vitro to an adjacent binding site that slightly overlaps UAS_p2 (data not shown).

Deletions in the PHO2-binding region ($\Delta 15$ and $\Delta 16$) showed no or only a minor decrease of *PHO5* mRNA expression in vivo (24). The same deletions, however, showed a drastic effect in vitro, since PHO2 binding was completely abolished. An explanation for these conflicting results is that because of the shortened distance between $\Delta 15$ and $\Delta 16$ in the two PHO4-binding sites, gene activation may

become independent of PHO2, since the PHO4 protein now directly interacts without need for the PHO2 protein. However, since the two deletion mutants $\Delta 15$ and $\Delta 16$ still depend on PHO2 in vivo (data not shown), this latter explanation is impossible.

It was recently shown that PHO2 is involved not only in phosphatase gene regulation but also in regulation of the basal level of *HIS4* (3). The authors gave an approximate localization of the PHO2 (BAS2)-binding site on the *PHO5* promoter by using the gel retardation assay. Moreover, it was shown that PHO2 is involved in the basal expression of *CYC1* (26). Furthermore, we have shown that PHO2 binds specifically to the *TRP4* promoter (Braus et al., in press). In the latter case, PHO2 is not essential for basal level expression of *TRP4* but clearly modulates the general control response of *TRP4*. Interestingly, the in vitro binding of PHO2 to the *TRP4* promoter is much stronger than the binding to the *PHO5* promoter, resulting in a very clear footprint pattern.

Unlike the PHO2 protein, PHO4 seems to be a specific regulator of the repressible phosphatase genes. Comparisons between UAS_p1 and UAS_p2 revealed a short sequence, CACGT, common to both UASs. Furthermore, this sequence is also found in the *PHO11* (24) and *PHO8* (12)

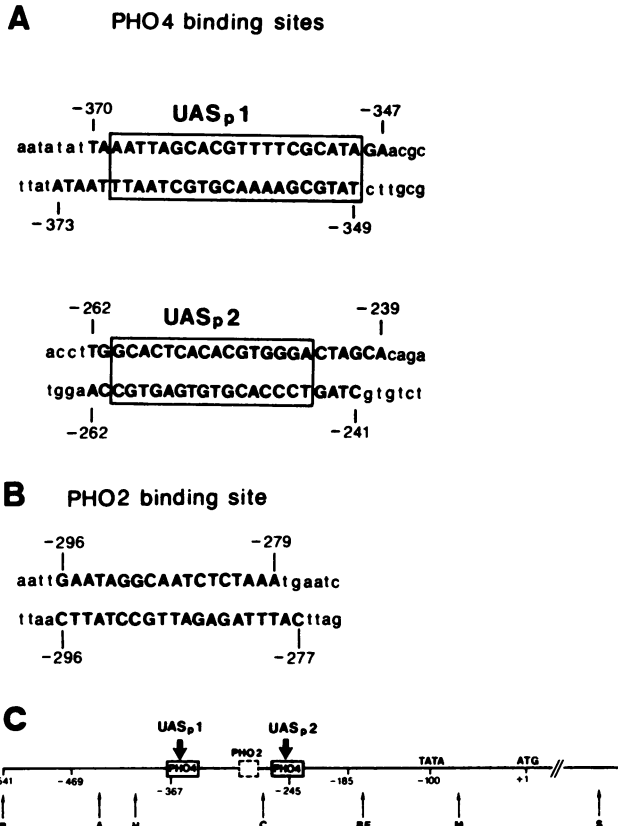


FIG. 6. Summary of PHO4- and PHO2-binding sites defined by DNase I and exonuclease III footprinting. (A) PHO4-binding sites. Sequences protected against DNase I digestion are indicated by bold capital letters; exonuclease III footprints are boxed. (B) PHO2-binding site. The DNase I-protected region is shown in bold capital letters. (C) Arrangement of UAS_{p1}, UAS_{p2}, and the PHO2-binding site on the *PHO5* promoter. Restriction sites are as described in the legend to Fig. 1.

promoter regions. All of these genes depend on PHO4 for activation. It is most likely that this sequence corresponds to the core sequence of the PHO4-binding element.

Studies of the regulation of *CYC1* have shown that binding of HAP1 in vitro, like the activity of UAS1 in vivo, is stimulated by heme (21, 22). GAL4, on the other hand requires zinc for binding to DNA in vitro and in vivo (11). We therefore asked whether PHO4 or PHO2 binding is influenced by certain low-molecular-weight factors and investigated the binding behavior in the presence of P_i, ATP, cAMP, and zinc ions. None of these components produced any changes in binding properties (data not shown).

We have compared different in vivo data, obtained by deletion mapping (7, 19, 24), with our in vitro data. The UAS_I (-382 to -391) and UAS_{II} (-332 to -341) proposed by Bergman et al. (6) do not coincide with our UASs obtained by DNase I and exonuclease III footprinting (Fig. 6A). Also, UAS II (-301 to -340) proposed by Nakao et al. (19) does not coincide with our UASs. However, the UAS I (-354 to -390) partially overlaps our UAS_{p1} (-347 to -373). Neither group found the element at -239 to -262 (UAS_{p2}) (Fig. 6A and C), which we show to be important for both *PHO5* activation in vivo and binding in vitro (24; this study). These divergent results could be attributable to the fact that Bergman et al. (6) and Nakao et al. (19) used quite large deletions for the localization of regulatory elements.

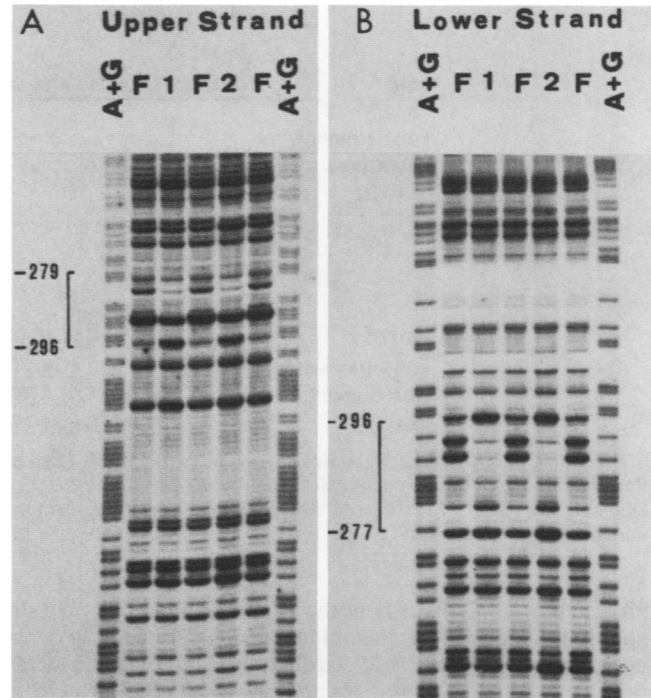


FIG. 7. DNase I footprint analysis with PHO2. DNase I footprinting was performed as described in Materials and Methods. The upper and lower strands of the *AatII-BstEII* restriction fragment were labeled as described in the legend to Fig. 4. The DNA probes were incubated with the PHO2 protein, digested with DNase I, and electrophoresed on a native polyacrylamide gel. The free DNA band, complex 1, and complex 2 were isolated, and the DNA was analyzed on a standard sequencing gel. A+G, Maxam-Gilbert sequencing reactions (18) used as size markers. Protected regions are bracketed on the left of each panel.

For some deletions used by Bergman et al. (6), the decreased activity appears to have been directly related to the lengths of the deletions. Furthermore, their studies were all done on multicopy plasmids, whereas the deletion studies by Rudolph and Hinnen (24) were done on integrated gene copies. The PHO4 data presented here are in good agreement with the data presented by Rudolph and Hinnen (24) (summarized in Fig. 8). Both $\Delta 11$ and $\Delta 12$, which caused a 10-fold decrease of *PHO5* mRNA, affect part of the PHO4-binding sequence determined by footprinting. Also, $\Delta 17$, which showed a fivefold decrease in *PHO5* mRNA (24), deletes important sequences for PHO4 binding.

In comparisons of our data with the chromatin structure of the *PHO5* promoter (2), it is interesting that UAS_{p1} coincides with a hypersensitive region that is observed independent of gene activation. This finding suggests that UAS_{p1} is not protected by a nucleosome and may always be available for protein-DNA interactions. Also, it is conceivable that the PHO4 protein is not the only regulator protein interacting with UAS_{p1}; it is possible that PHO80, the negative factor for the repressible *PHO5* gene, binds to the same or an overlapping sequence, as has recently been suggested by Madden et al. (16). In comparison, experiments with the *CYC1* promoter have shown that the *HAP1* activator not only requires heme for optimal binding to UAS1 but also competes with the factor RC2 for the same binding site (21).

The interaction of the PHO2 protein with the *PHO5* promoter cannot be explained readily, since the PHO2

- 65:499-560.
19. Nakao, J., A. Miyahara, A. Toh-e, and K. Matsubara. 1986. *Saccharomyces cerevisiae* *PHO5* promoter region: location and function of the upstream activation site. *Mol. Cell. Biol.* **6**: 2613-2623.
 20. Parent, S. A., A. G. Tait-Kamradt, J. LeVitre, O. Lifanova, and K. A. Bostian. 1987. Regulation of the phosphatase multigene family of *Saccharomyces cerevisiae*, p. 63-70. In A. Torriani-Gorini, F. G. Rothman, S. Silver, A. Wright, and E. Yagil (ed.), *Phosphate metabolism and cellular regulation in microorganisms*. American Society for Microbiology, Washington, D.C.
 21. Pfeifer, K., B. Arcangioli, and L. Guarente. 1987. Yeast HAP1 activator competes with the factor RC2 for binding to the upstream activation site UAS1 of the *CYC1* gene. *Cell* **49**:9-18.
 22. Pfeifer, K., T. Prezant, and L. Guarente. 1987. Yeast HAP1 activator binds to two upstream activation sites of different sequence. *Cell* **49**:19-27.
 23. Remaut, E., P. Stanssens, and W. Fiers. 1981. Plasmid vectors for high-efficiency expression controlled by the P_L promoter of coliphage lambda. *Gene* **15**:81-93.
 24. Rudolph, H., and A. Hinnen. 1987. The yeast *PHO5* promoter: phosphate-control elements and sequences mediating mRNA start-site selection. *Proc. Natl. Acad. Sci. USA* **84**:1340-1344.
 25. Sengstag, C., and A. Hinnen. 1987. The sequence of the *Saccharomyces cerevisiae* gene *PHO2* codes for a regulatory protein with unusual aminoacid composition. *Nucleic Acids Res.* **15**:233-246.
 26. Sengstag, C., and A. Hinnen. 1988. A 28 bp segment of the *S. cerevisiae* *PHO5* UAS confers phosphate control to the heterologous gene *CYC1-lacZ*. *Gene* **67**:223-228.